Different shades of a molecular dance - foundations and applications of FT-IR microscopy in biophysics

Artur D. Surowka, Dr inż.
email : asurowka@agh.edu.pl

AGH University of Science and Technology
Faculty of Physics and Applied Computer Science
Department of Medical Physics and Biophysics

July 17^{th}, 2020

Table of contents

In this lecture, You will learn some basics of FT-IR microscopy,

- A glimpse of theory
- Highlight into current FT-IR microscopy instrumentation
- Current applications

Infrared radiation - low energy, high significance!

The IR spectrum in brief

The IR spectrum radiation is a region of the electromagnetic spectrum for wavelengths ranging from 700 nm - 1 mm.

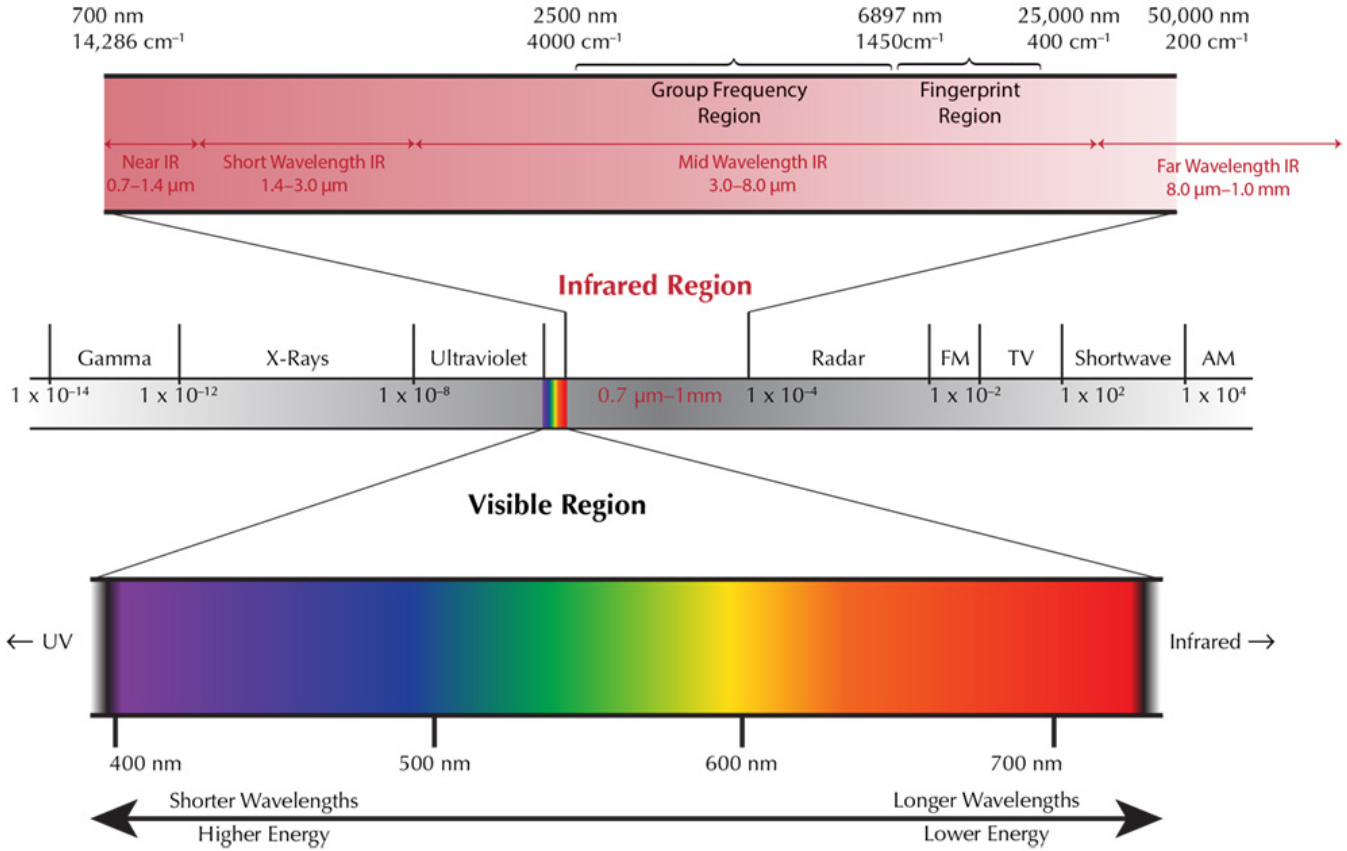

Fig. 1: The IR spectrum [1]

Foundations of vibrational spectroscopy

Molecule as a simple **harmonic oscillator**.

In all, IR spectroscopy is a powerful technique based on the vibrations of the atoms of an molecule. An IR spectrum is obtained by passing infrared radiation thorough the sample and calculating what the fraction of incident beam is absorbed at particular energy [9].

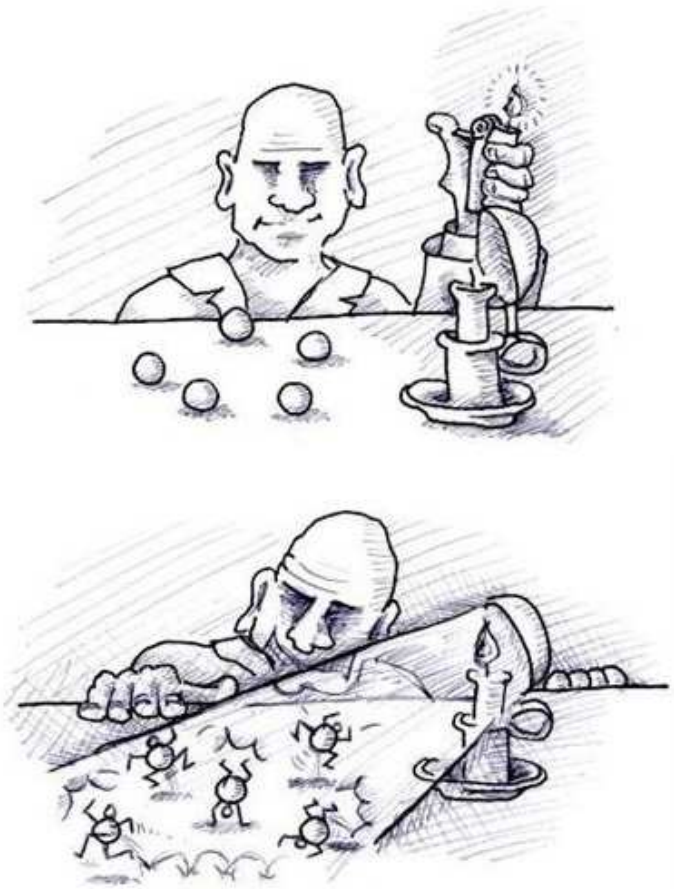

Fig. 2: "Molecular dance" - unknown artist ;).

Foundations of vibrational spectroscopy

Molecule as a simple **harmonic oscillator**.

According to the basic model, a molecule can be treated as a system of masses joined by chemical bonds with "spring-like" properties, namely it is so-called **harmonic oscillator**. Each harmonic oscillator is allowed to perform 3N-5 (linear molecules) or 3N-6 (non-linear molecules) modes of vibrations [7].

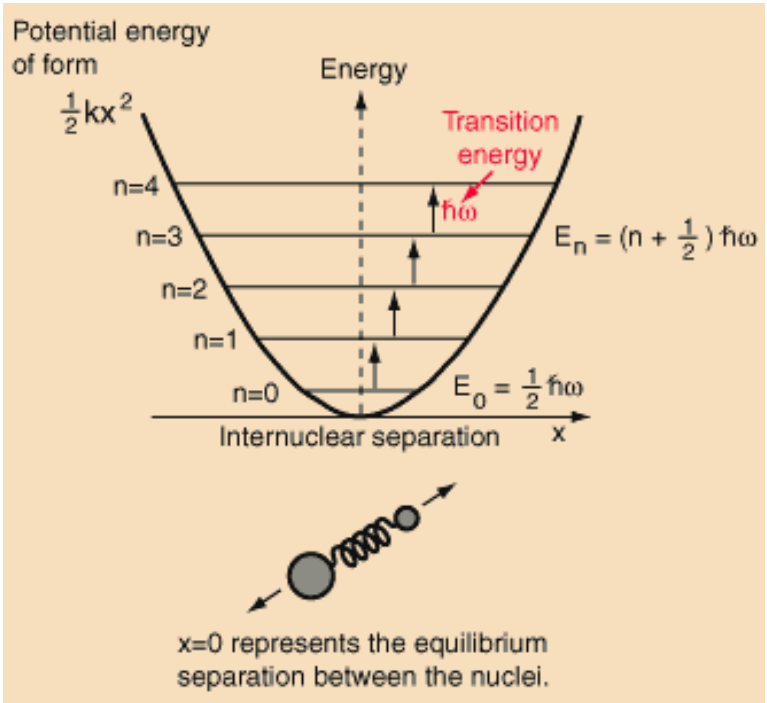

Fig. 2: Potential energy of a diatomic molecule as a function of the atomic displacement during vibrations of a simple harmonic oscillator [2].

Foundations of vibrational spectroscopy

Molecule as a simple **harmonic oscillator**.

For any mode in which atoms vibrate with simple harmonic motion (i.e. obeying Hooke's law), the vibrational energy states can be described by simple equation (famous solution of Schrodinger's equation for simple harmonic oscillator): [7]

$$V(v_i) = h\nu_i \left(v_i + \frac{1}{2} \right) \qquad (1)$$

Where:
- v_i - vibrational quantum number of i-th mode of vibration, where: $v_i = 0, 1, 2...$,
- ν_i - fundamental frequency of a given vibration [Hz] (typically, (for MIR) in order of 10^{13} [Hz] (0.2 eV)).

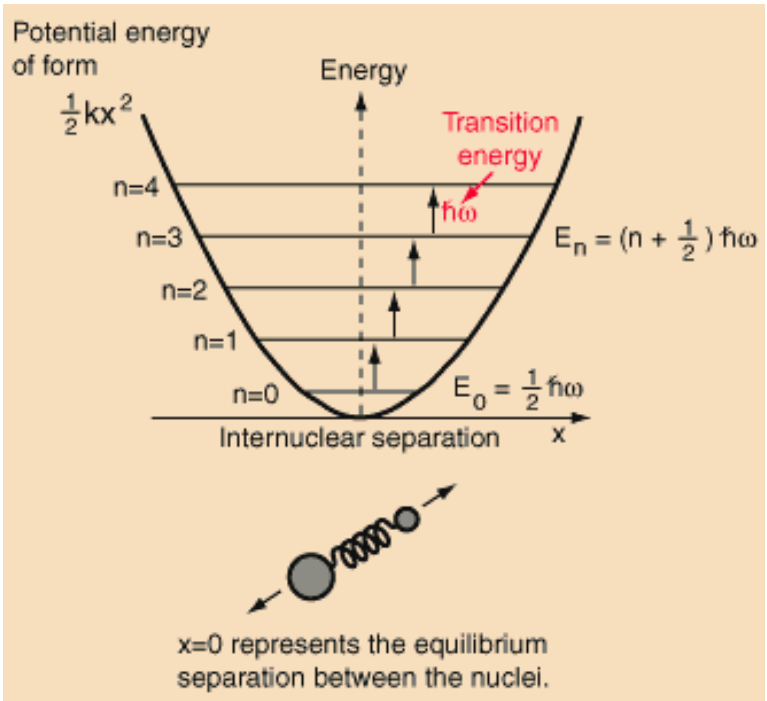

Fig. 2: Potential energy of a diatomic molecule as a function of the atomic displacement during vibrations of a simple harmonic oscillator [2].

Foundations of vibrational spectroscopy

Molecule as a simple **harmonic oscillator**.

$$V(v_i) = h\nu_i \left(v_i + \frac{1}{2} \right) \qquad (1)$$

Where:
- v_i - vibrational quantum number of i-th mode of vibration, where: $v_i = 0, 1, 2...$,
- ν_i - fundamental frequency of a given vibration [Hz] (typically, (for MIR) in order of 10^{13} [Hz] (0.2 eV)).

Based on the selection rules for simple harmonic oscillator, all transitions involving changes in v_i by ± 1 would be allowed [7]!!!

Hence:

$$\Delta v_i = \pm 1 \qquad (2)$$

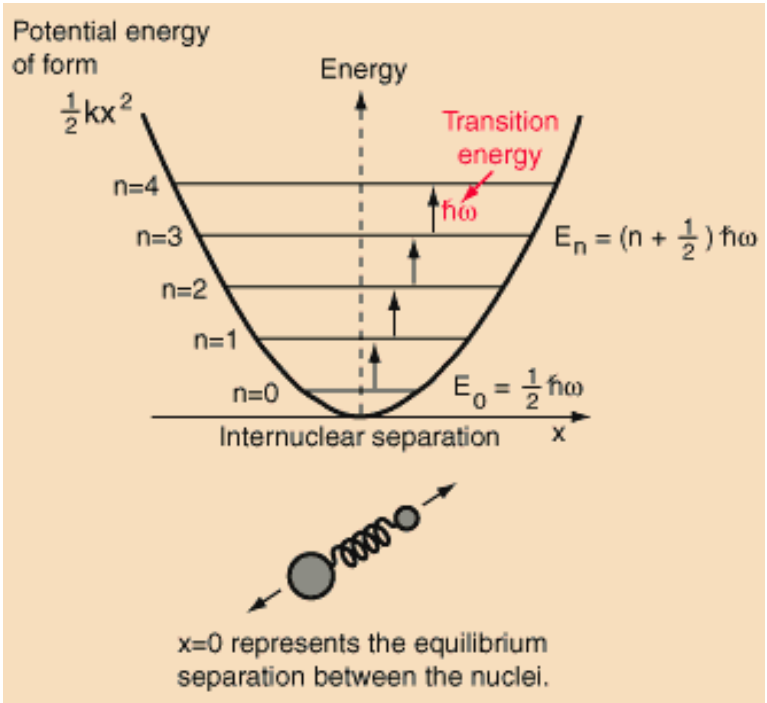

Fig. 2: Potential energy of a diatomic molecule as a function of the atomic displacement during vibrations of a simple harmonic oscillator [2].

Normal modes of vibration

Basics steps in a molecular dance

Except from selection rules, additional condition has to be fulfilled, namely the molecule is only promoted to the excited state if its dipole moment, μ_m, changes during the vibration, hence for transitions between ground level and higher we may write:

$$B_{0i} \approx \left(\frac{d\mu}{dq}\right)^2 \qquad (3)$$

Where:
- μ - dipole moment of a given molecule [7].

Permanent dipole moment must change due to vibrational motion of oscillator for the vibration to be capable of absorbing an IR photon [7]!!!!

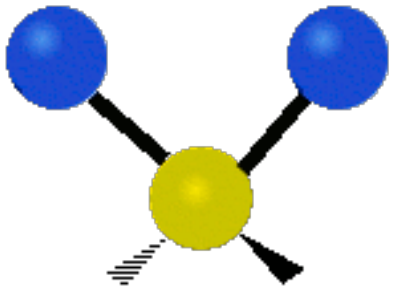

(a) $\nu_s \approx 2920cm^{-1}$.

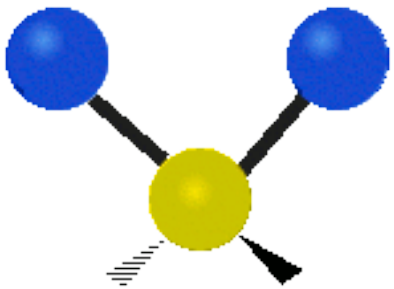

(b) $\nu_{as} \approx 2850cm^{-1}$

Fig. 3: Various modes of vibration for $-CH_2-$ group: (a) symmetric stretching (b) antisymmetric stretching [3].

Normal modes of vibration

Basics steps in a molecular dance

Except from selection rules, additional condition has to be fulfilled, namely the molecule is only promoted to the excited state if its dipole moment, μ_m, changes during the vibration, hence for transitions between ground level and higher we may write:

$$B_{0i} \approx \left(\frac{d\mu}{dq}\right)^2 \qquad (3)$$

Where:
- μ - dipole moment of a given molecule [7].

Permanent dipole moment must change due to vibrational motion of oscillator for the vibration to be capable of absorbing an IR photon [7]!!!!

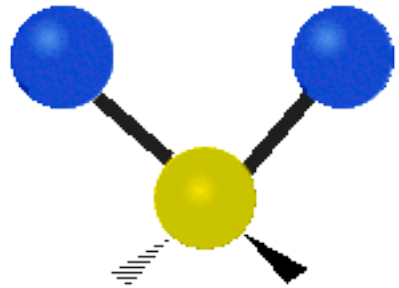

(a) $\delta \approx 1470cm^{-1}$.

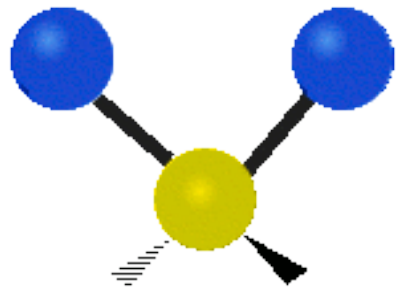

(b) $\tau \approx 1370cm^{-1}$

Fig. 3: Various modes of vibration for $-CH_2-$ group: (a) bending (b) twisting [3].

Normal modes of vibration

Basics steps in a molecular dance

Except from selection rules, additional condition has to be fulfilled, namely the molecule is only promoted to the excited state if its dipole moment, μ_m, changes during the vibration, hence for transitions between ground level and higher we may write:

$$B_{0i} \approx \left(\frac{d\mu}{dq}\right)^2 \qquad (3)$$

Where:
- μ - dipole moment of a given molecule [7].

Permanent dipole moment must change due to vibrational motion of oscillator for the vibration to be capable of absorbing an IR photon [7]!!!!

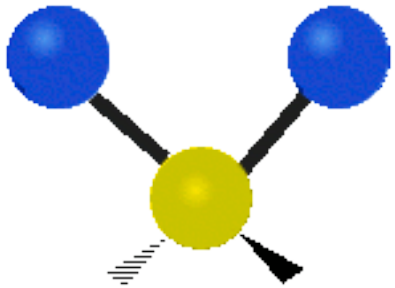

(a) $\rho \approx 720cm^{-1}$.

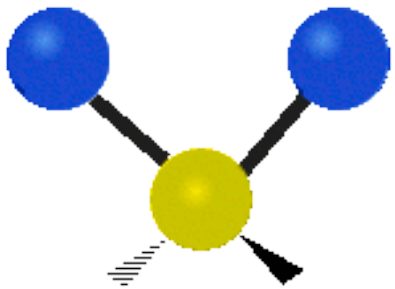

(b) $\omega \approx 1350 - 180cm^{-1}$

Fig. 3: Various modes of vibration for $-CH_2-$ group: (a) rocking (b) wagging [3].

Foundations of vibrational spectroscopy

Molecule as an **anharmonic oscillator** - is it more freestyle?.

Real molecules are not perfect harmonic oscillators since force constant of a chemical bond is not constant for molecular vibrations of different amplitude. It turns out that V_i must be described using an anharmonic, i.e. Morse-type potential function ($q_e = 0$):

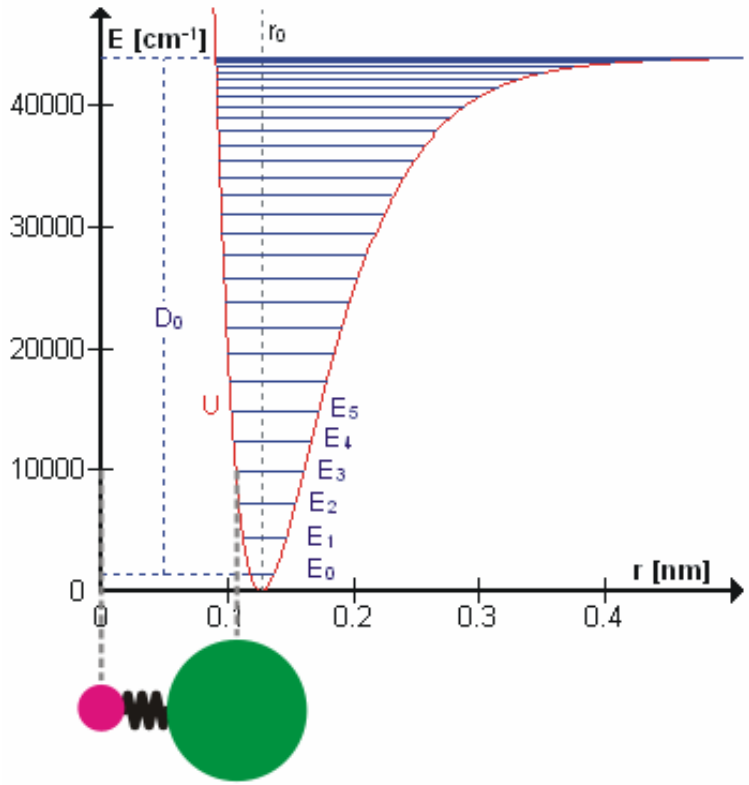

Fig. 4: Potential energy of a diatomic molecule as a function of the atomic displacement during vibrations of an aharmonic oscillator [3].

Foundations of vibrational spectroscopy

Molecule as an **anharmonic oscillator** - is it more freestyle?.

Real molecules are not perfect harmonic oscillators since force constant of a chemical bond is not constant for molecular vibrations of different amplitude. It turns out that V_i must be described using an anharmonic, i.e. Morse-type potential function ($q_e = 0$):

$$U(q) = D\left(1 - e^{-\beta \cdot q}\right)^2 \qquad (4)$$

Where:
- D - potential well depth,
- β - the factor describing "curvature" of the potential [9].

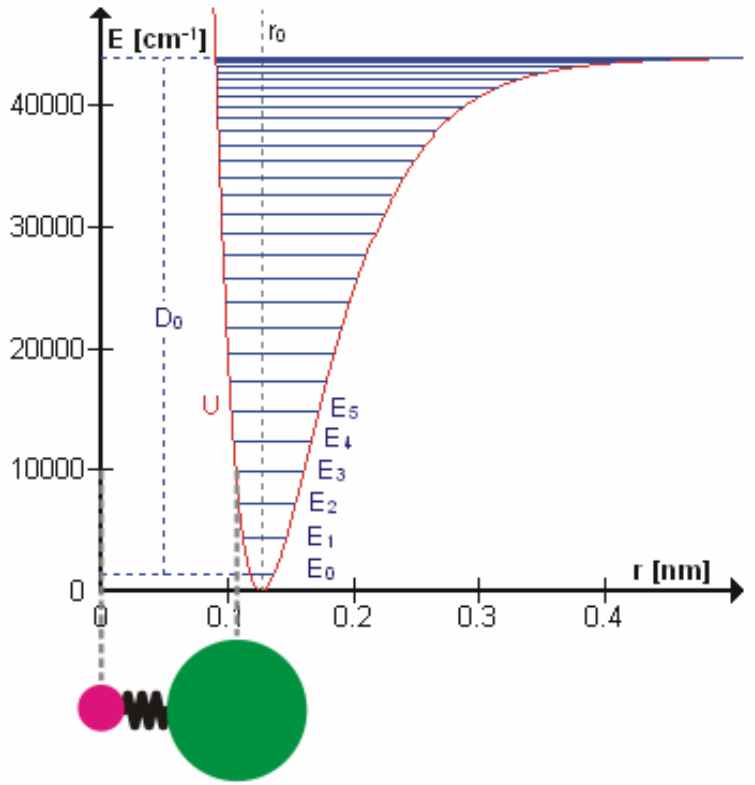

Fig. 4: Potential energy of a diatomic molecule as a function of the atomic displacement during vibrations of an aharmonic oscillator [3].

Foundations of vibrational spectroscopy

Molecule as an **anharmonic oscillator** - is it more freestyle?.

$$U(q) = D\left(1 - e^{-\beta \cdot q}\right)^2 \qquad (4)$$

Where:
- D - potential well depth,
- β - the factor describing "curvature" of the potential [9].

Based on the Schrodinger equation, applied for a "Morse-like" potential, the eigen value of energy of an anharmonic oscillator is given the formula presented below:

$$E_i = h\nu_i\left(v_i + \frac{1}{2}\right) - h\nu_i x_i\left(v_i + \frac{1}{2}\right)^2 \qquad (5)$$

Where:
- ν_i, v_i - as in eq. 2,
- x_i - the anharmonicity constant; usually: $0.001 < x_i < 0.02$ [9].

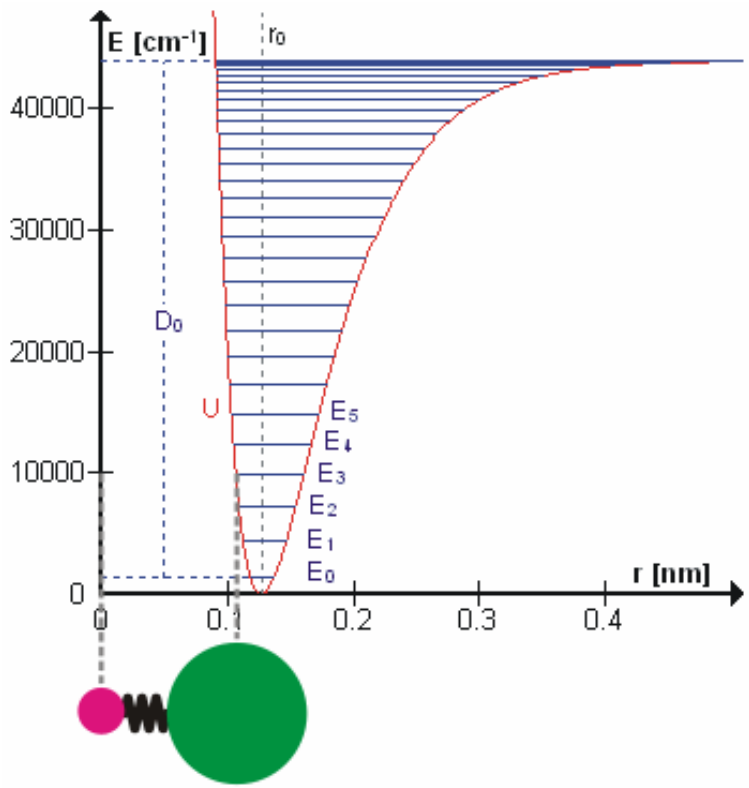

Fig. 4: Potential energy of a diatomic molecule as a function of the atomic displacement during vibrations of an aharmonic oscillator [3].

Foundations of vibrational spectroscopy

Molecule as an **anharmonic oscillator** - is it more freestyle?.

$$E_i = h\nu_i \left(v_i + \frac{1}{2}\right) - h\nu_i x_i \left(v_i + \frac{1}{2}\right)^2 \quad (4)$$

Where:
- ν_i, v_i - as in eq. 2,
- x_i - the anharmonicity constant; usually: $0.001 < x_i < 0.02$ [9].

The effect of anharmonicity is to relax selection rules for harmonic oscillator.

Therefore, transitions involving:

$$\Delta v_i = \pm 1, \pm 2, \pm 3, \ldots \quad (5)$$

become allowed [7]!

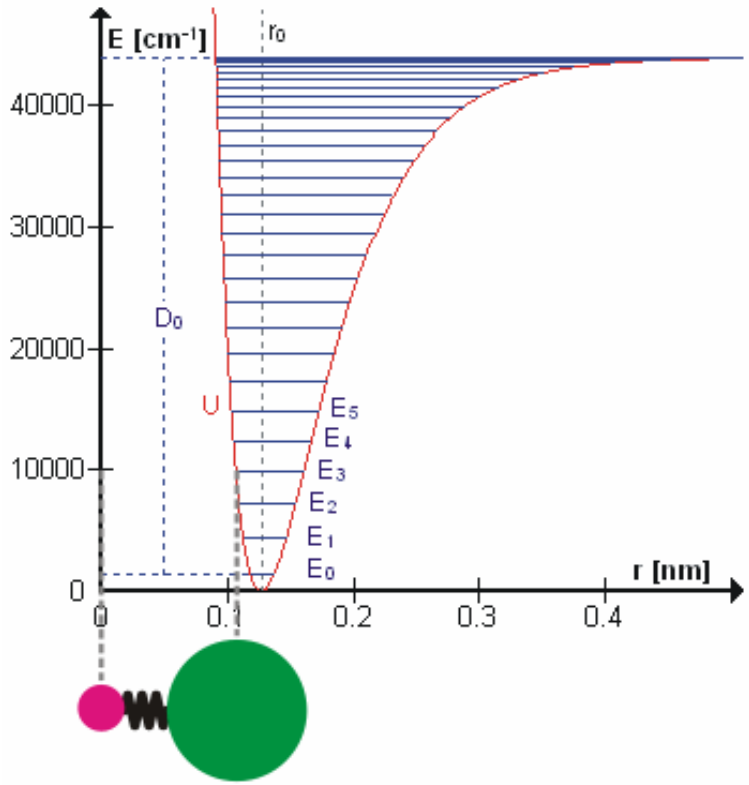

Fig. 4: Potential energy of a diatomic molecule as a function of the atomic displacement during vibrations of an aharmonic oscillator [3].

Instrumentation for FT-IR microscopy

How to measure FT-IR spectra

It can be interesting to measure how much of the incident IR radiation gets absorbed at specific wavelengths as it they pass through a sample!!!!

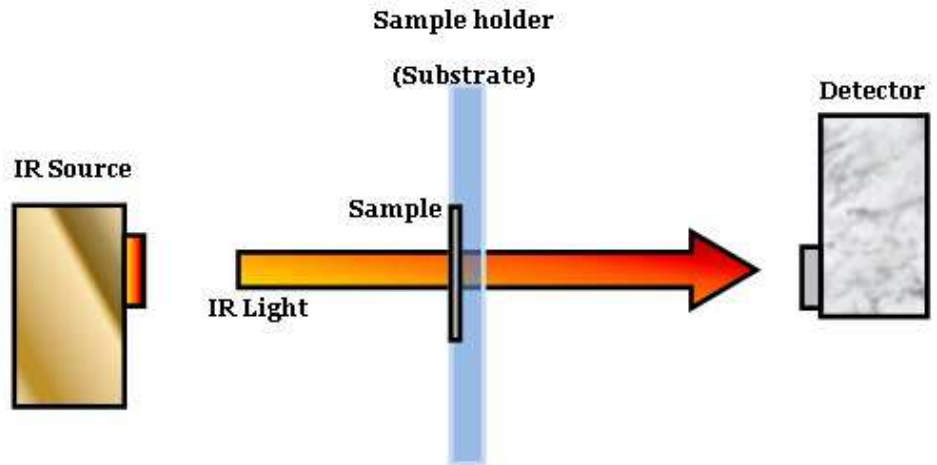

Fig. 5: Idea of transmission IR experiments [8].

It can be interesting to measure it as absorbance:

$$A(\tilde{\nu}) = log(\frac{I(\tilde{\nu})}{I_0(\tilde{\nu})}) = \epsilon c l \text{ and } \tilde{\nu} = \frac{2\pi}{\lambda} \quad (6)$$

Where: I_0 - the intensity of the "reference" (background), I - intensity of the attenuated radiation; ϵ - molar absorptivity $[dm^3/(mol \cdot cm)]$; c - concentration $[mol/dm^3]$; l - path-length $[cm]$.

Instrumentation for FT-IR microscopy

How Michelson Interferometer works?

The interferogram of a collimated beam of monochromatic radiation of intensity $I(\tilde{\nu_0})$ at wavenumber $\tilde{\nu_0}$ at an optical path difference δ is given by following equation:

$$I(\delta) = 0.5 \cdot I(\tilde{\nu_0}) \cdot cos(2\pi\tilde{\nu_0}\delta) \quad (7)$$

To obtain the true spectrum $B(\tilde{\nu})$, the cosine FT must be calculated from equation:

$$B(\tilde{\nu}) = \int_{-\infty}^{+\infty} I(\delta) \cdot D(\delta) \cdot cos(2\pi\tilde{\nu}\delta) d\delta \quad (8)$$

Where:
- $D(\delta)$ - so-called apodization function (i.e. "box-car", triangular, Happ-Genzel, etc.) [9, 7, 4].

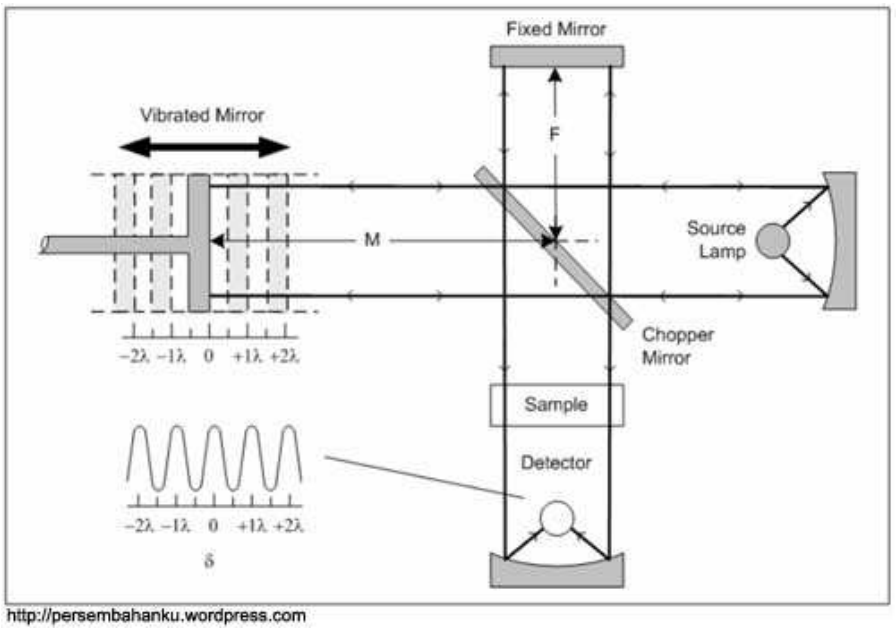

Fig. 6: Schematic of a FTIR Michelson interferometer [5].

Instrumentation for FT-IR microscopy

How Michelson Interferometer works?

The interferogram of a collimated beam of monochromatic radiation of intensity $I(\tilde{\nu_0})$ at wavenumber $\tilde{\nu_0}$ at an optical path difference δ is given by following equation:

$$I(\delta) = 0.5 \cdot I(\tilde{\nu_0}) \cdot cos(2\pi\tilde{\nu_0}\delta) \quad (7)$$

To obtain the true spectrum $B(\tilde{\nu})$, the cosine FT must be calculated from equation:

$$B(\tilde{\nu}) = \int_{-\infty}^{+\infty} I(\delta) \cdot D(\delta) \cdot cos(2\pi\tilde{\nu}\delta) d\delta \quad (8)$$

Where:
- $D(\delta)$ - so-called apodization function (i.e. "box-car", triangular, Happ-Genzel, etc.) [9, 7, 4].

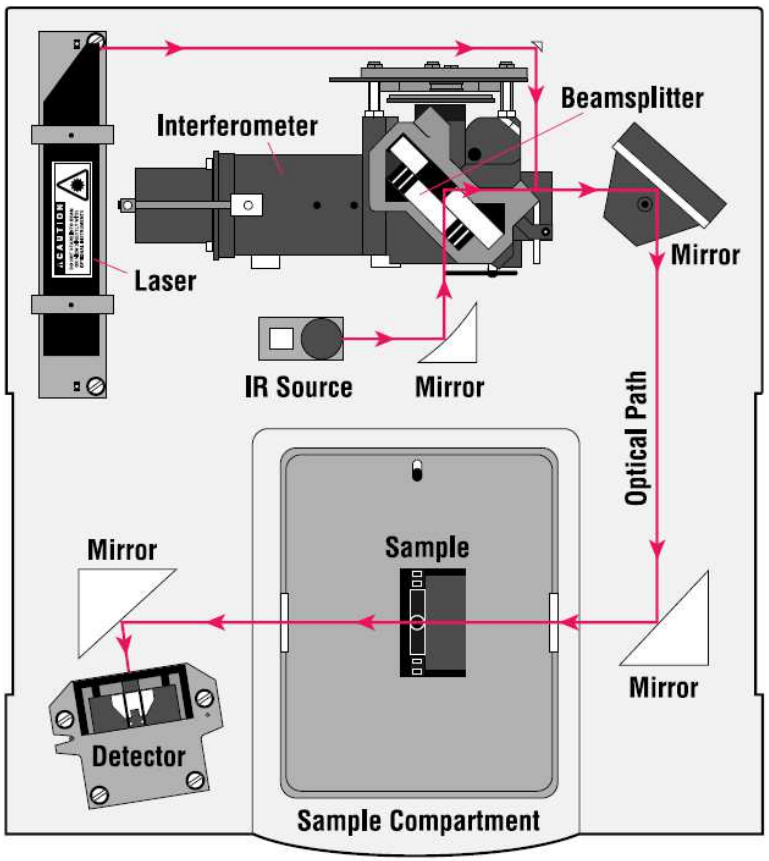

Fig. 6: Schematic of a FTIR Michelson interferometer [5].

Instrumentation for FT-IR microscopy

How Michelson Interferometer works?

The interferogram of a collimated beam of monochromatic radiation of intensity $I(\tilde{\nu_0})$ at wavenumber $\tilde{\nu_0}$ at an optical path difference δ is given by following equation:

$$I(\delta) = 0.5 \cdot I(\tilde{\nu_0}) \cdot cos(2\pi\tilde{\nu_0}\delta) \quad (7)$$

To obtain the true spectrum $B(\tilde{\nu})$, the cosine FT must be calculated from equation:

$$B(\tilde{\nu}) = \int_{-\infty}^{+\infty} I(\delta) \cdot D(\delta) \cdot cos(2\pi\tilde{\nu}\delta) d\delta \quad (8)$$

Where:
- $D(\delta)$ - so-called apodization function (i.e. "box-car", triangular, Happ-Genzel, etc.) [9, 7, 4].

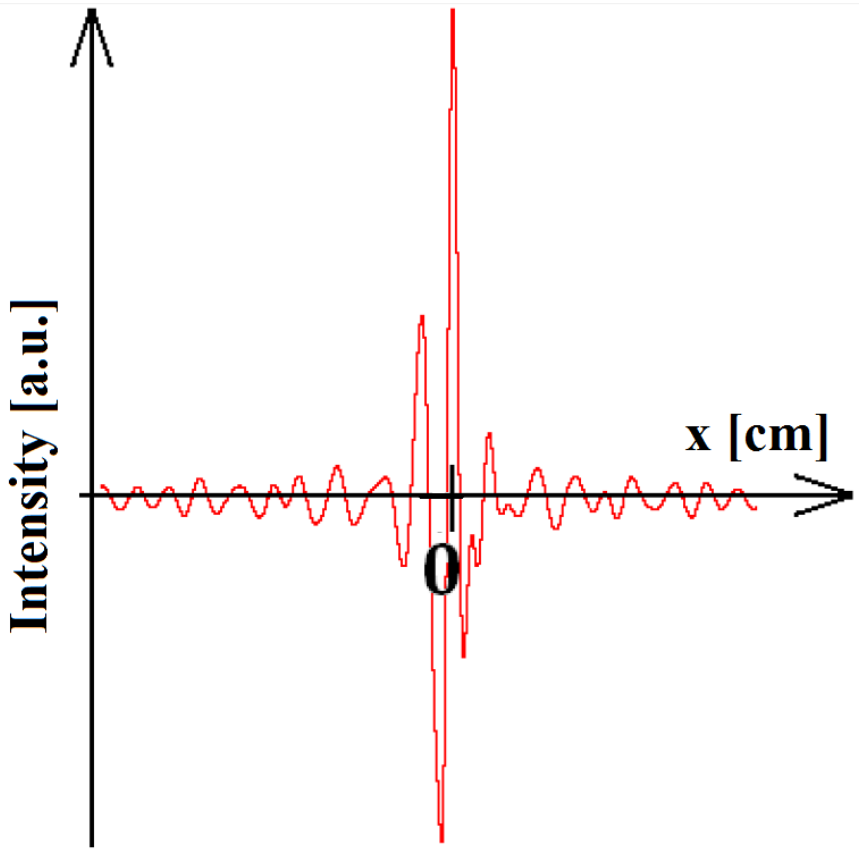

Fig. 6: Interferogram.

Instrumentation for FT-IR microscopy

FTIR spectrum of human tissue

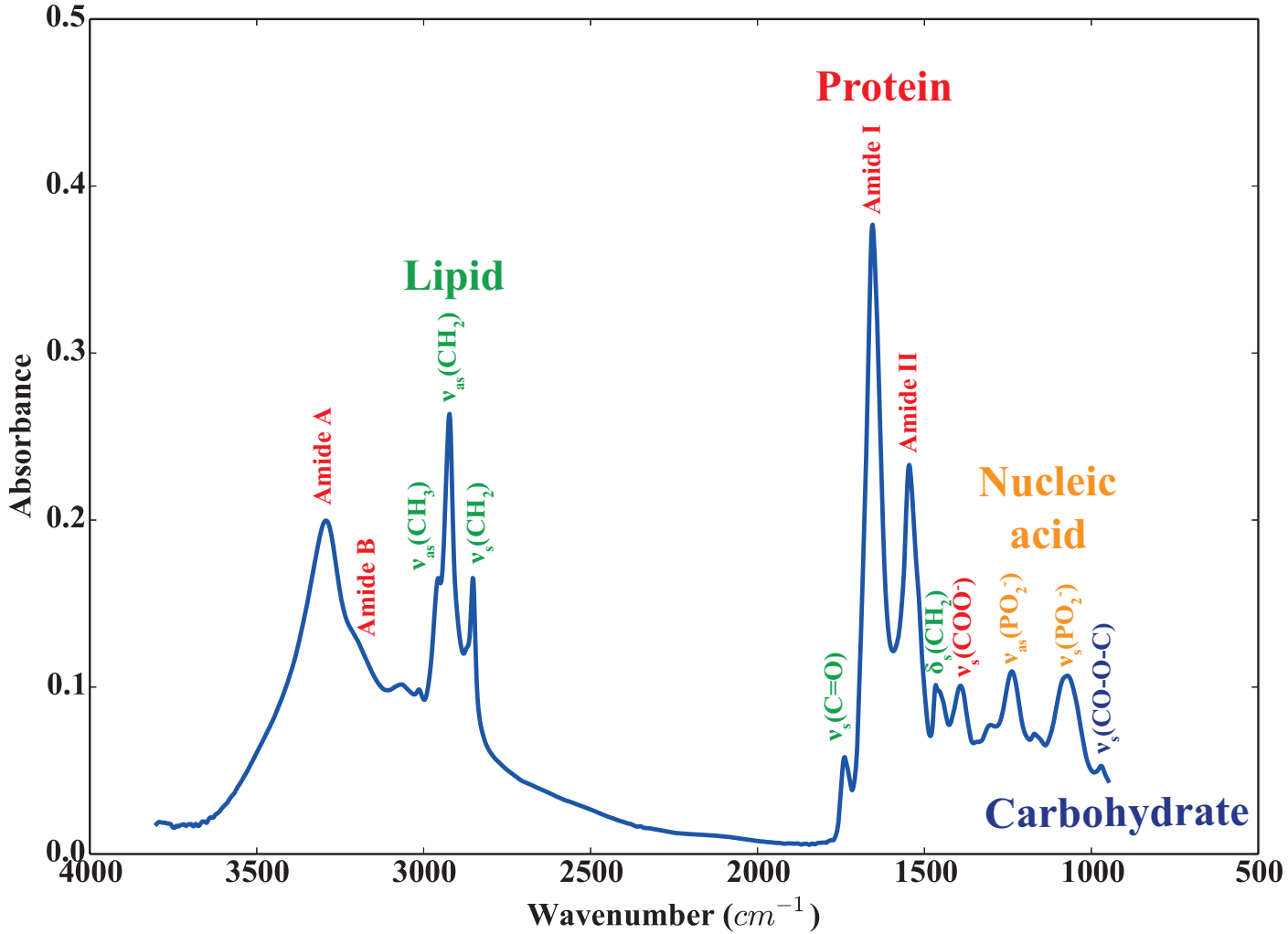

Fig. 7: FTIR spectrum of human brain tissue [10].

Measurement modalities

FTIR microscopy

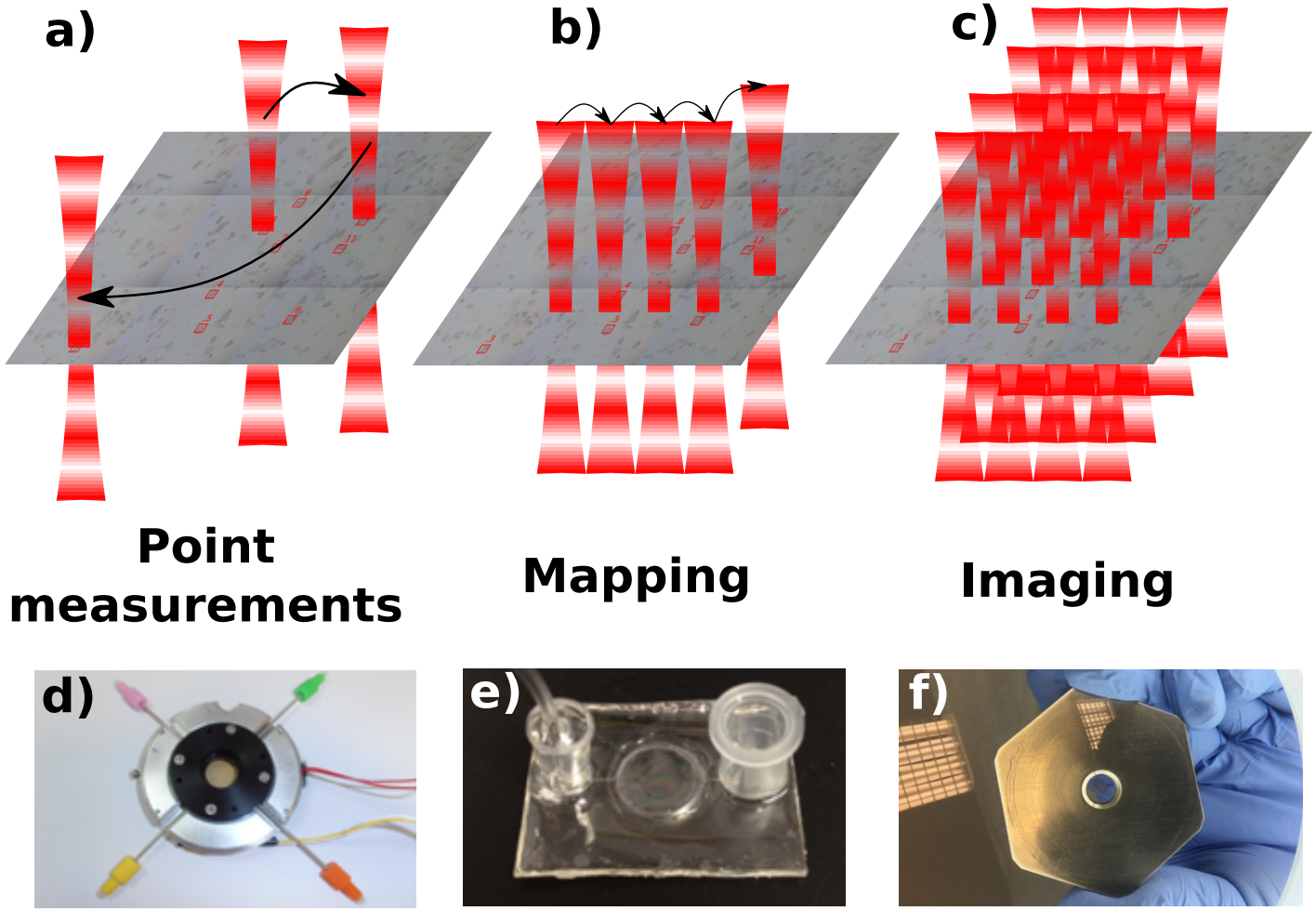

Fig. 8: Example measurement modalities in FT-IR microscopy: a) single point; b) raster scanning; c) imaging.

Glial tumors - proteins *vs* malignancy grade [11]

- **Background**: around 80% of malignant brain tumorous are gliomas. They are classified into four malignancy grades: I (benign) - IV (malignant) as proposed by the World Health Organization (WHO).
- **Aim**: discrimination between the glial tumors of various types and malignancy grades based on their protein secondary structure.
- **Methods**: SR-FTIR micro-spectroscopy (SMIS beamline, SOLEIL, Saint Aubin, France) + chemometrics (MATLAB + Python) involving the use of artificial neural networks (ANNs).
- **Objectives**: seeking the best training dataset, optimization of networks' topology, training, predictions.

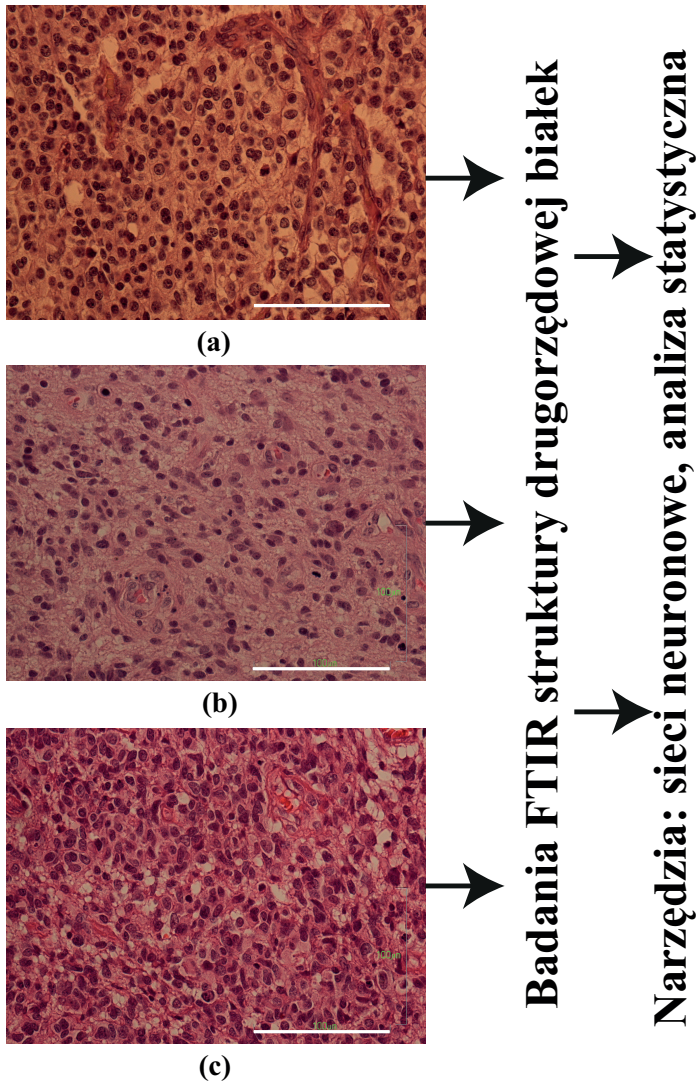

Fig. 9: Layout of the prediction procedure.

Glial tumors - proteins *vs* malignancy grade [11]

- **Background**: around 80% of malignant brain tumorous are gliomas. They are classified into four malignancy grades: I (benign) - IV (malignant) as proposed by the World Health Organization (WHO).
- **Aim**: discrimination between the glial tumors of various types and malignancy grades based on their protein secondary structure.
- **Methods**: SR-FTIR micro-spectroscopy (SMIS beamline, SOLEIL, Saint Aubin, France) + chemometrics (MATLAB + Python) involving the use of artificial neural networks (ANNs).
- **Objectives**: seeking the best training dataset, optimization of networks' topology, training, predictions.

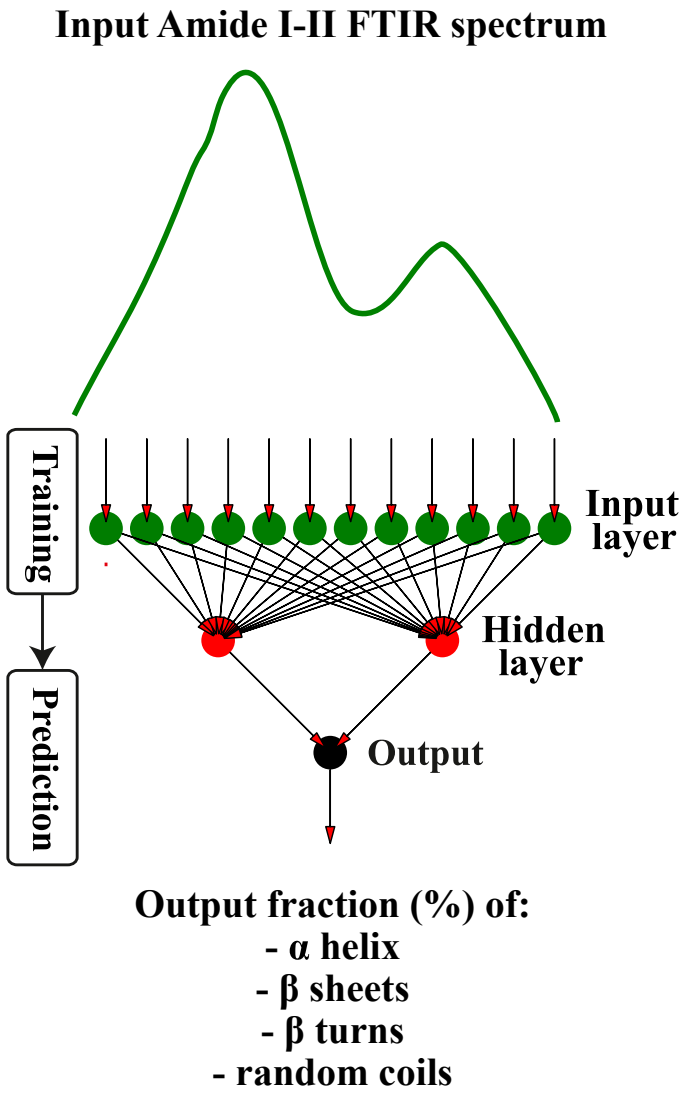

Fig. 9: Layout of the prediction procedure.

Glial tumors - proteins *vs* malignancy grade [11]

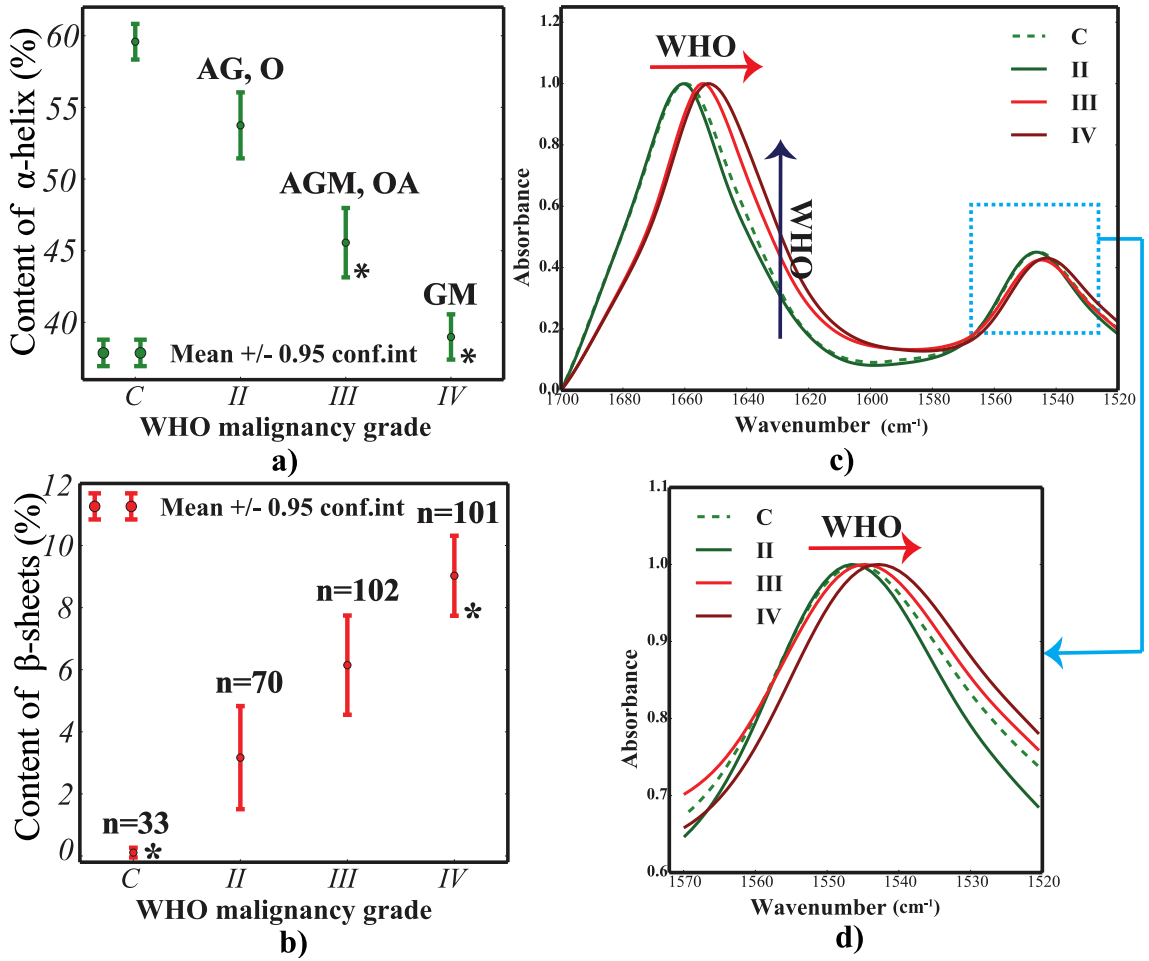

Fig. 10: Average values of protein secondary structure contents *vs* tumor's malignancy grade for: a) α-helices; b) β-sheets, respectively. c) Amide I-II spectra of the glial tumors, averaged over the malignancy grade, normalized to the maximum of amide I; d) amide II spectrum normalized to its maximum (the arrows show the increase in the malignancy grade).

Glial tumors - proteins *vs* malignancy grade [11]

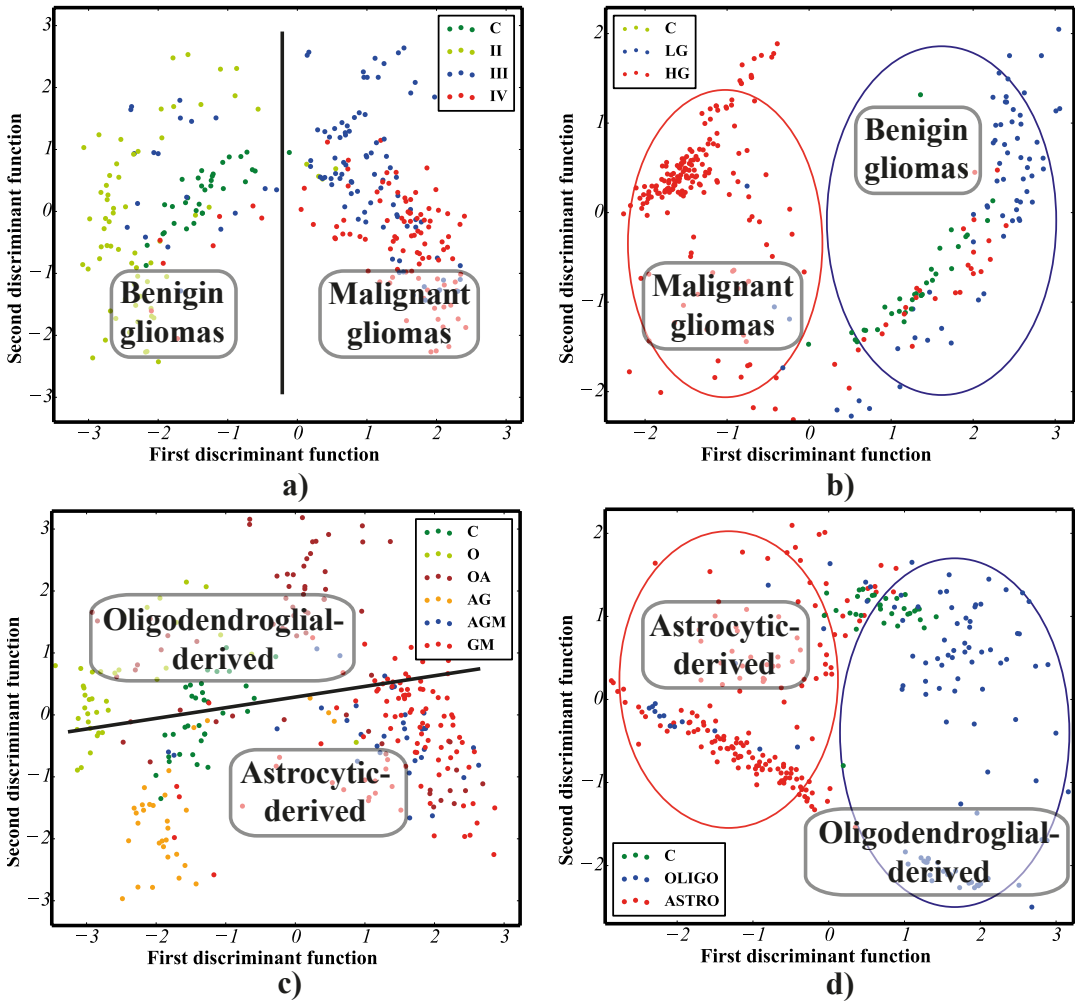

Fig. 10: Linear discriminant analysis (LDA): distribution of the data points in the space of discriminant functions for the classification with respect to: a) malignancy grade; b) general malignancy grade; c) histological origin; d) general histological origin.

Glial tumors - proteins *vs* malignancy grade [11]

Conclusions

a) Protein secondary structure in a tissue sample can be regarded as a general indicator of the glial tumor's malignancy or its histological origin.

b) The procedure involving ANNs and micro-SR-FTIR enabled precise predictions (SEP: 3-4%) of protein secondary contents.

c) However, because of the prediction time, the procedure needs to be accelerated (ongoing).

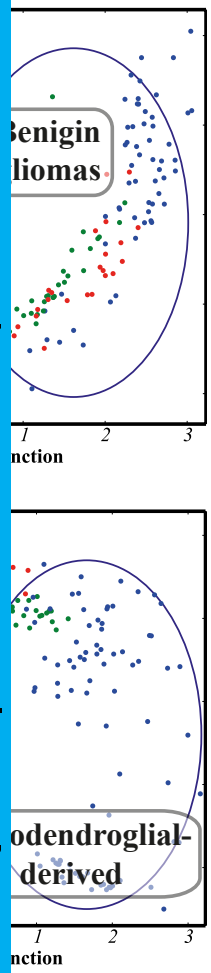

Fig. nts in the space of discriminant functions for the classification with respect to: a) malignancy grade, b) general malignancy grade; c) histological origin; d) general histological origin.

FT-IR imaging for neuro-research [13]

Protein burden in Alzheimer disease

- **Background**: $A\beta$ plaques are considered casual for neurodegeneration in Alzheimer disease (AD). However, their participation in early-stage pathologies is unknown.
- **Aim**: Characterization of local biochemical burden occurring in close proximity of $A\beta$ in the 3-Tg-APP-PS1-TAU mouse model of early-stage Alzheimer disease.
- **Methods**: FTIR imaging (Agilent Cary 620-IR imaging microscope: 128 x 128 matrix, pixel: 1.1 μm) and spectral band fitting.
- **Objectives**: development of the in-house code (Python) by image processing and chemometrics.

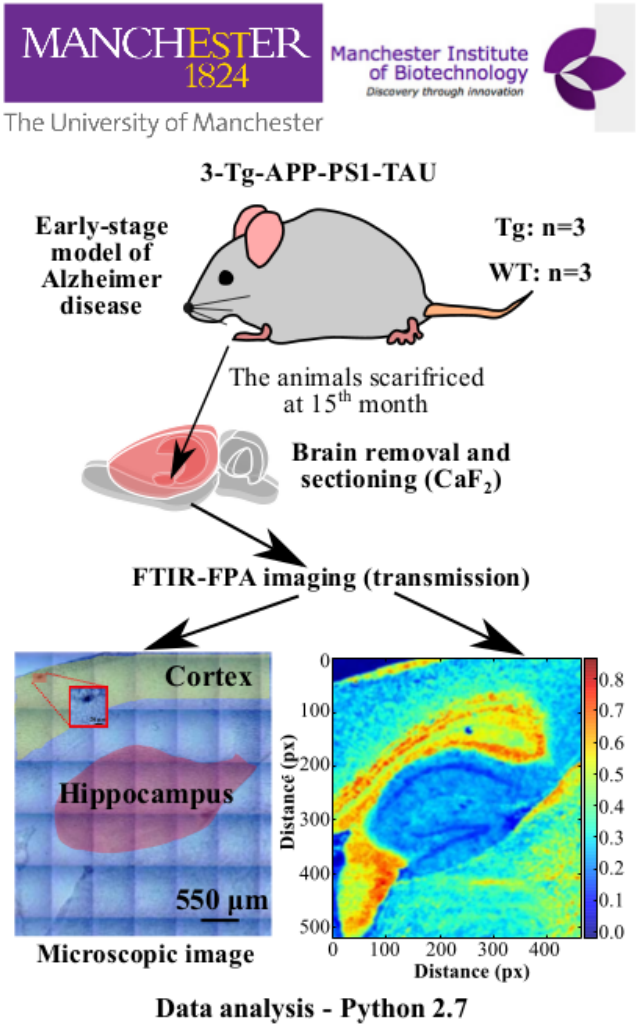

Fig. 11: Experimental outline.

FT-IR imaging for neuro-researc [13]

Data analysis

Amide I spectra were analyzed by the curve fitting approach. The fitting model was optimized to yield the best performance and sensitivity.

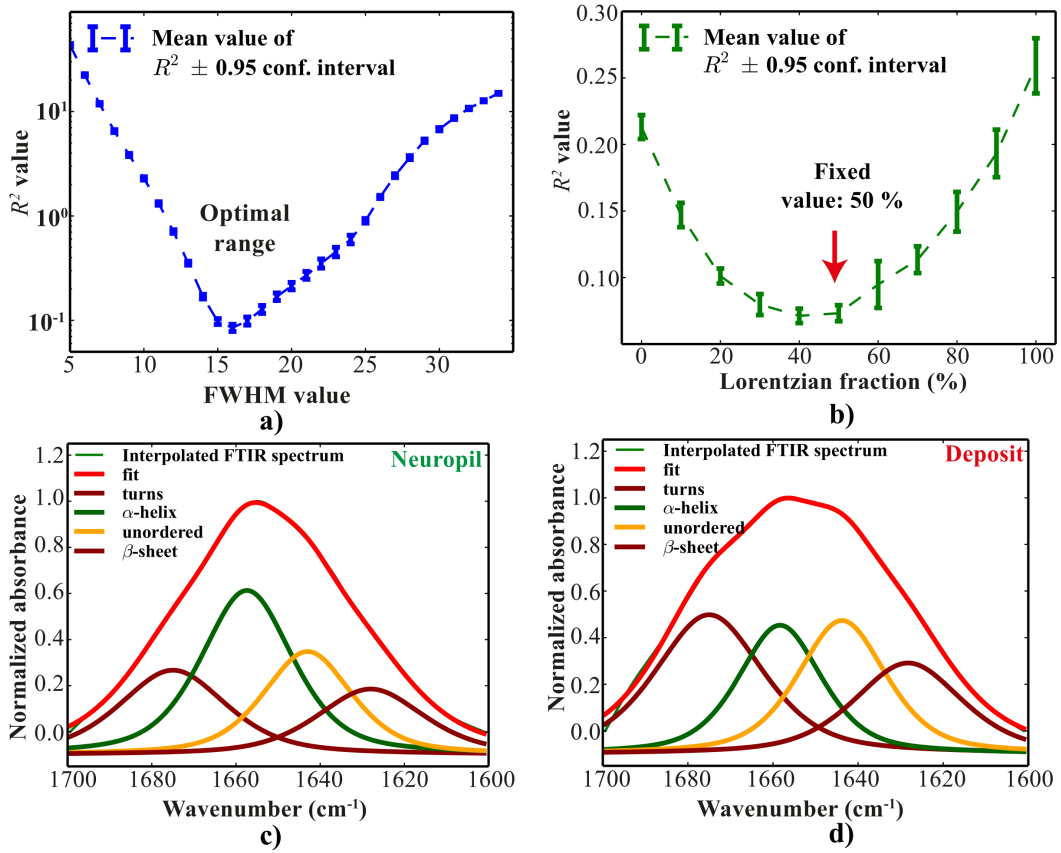

Fig. 12: The procedure for spectral band fitting: a) coefficient of determination *vs* peak FWHM value; b) coefficient of determination *vs* Lorentzian fraction in a peak; c-d) curve-fitted amide I spectra of the $A\beta$ and neuropil, respectively.

Image analysis and results [13]

Immediate areas around the identified $A\beta$ deposits were determined by image processing (in-house code implemented in Python).

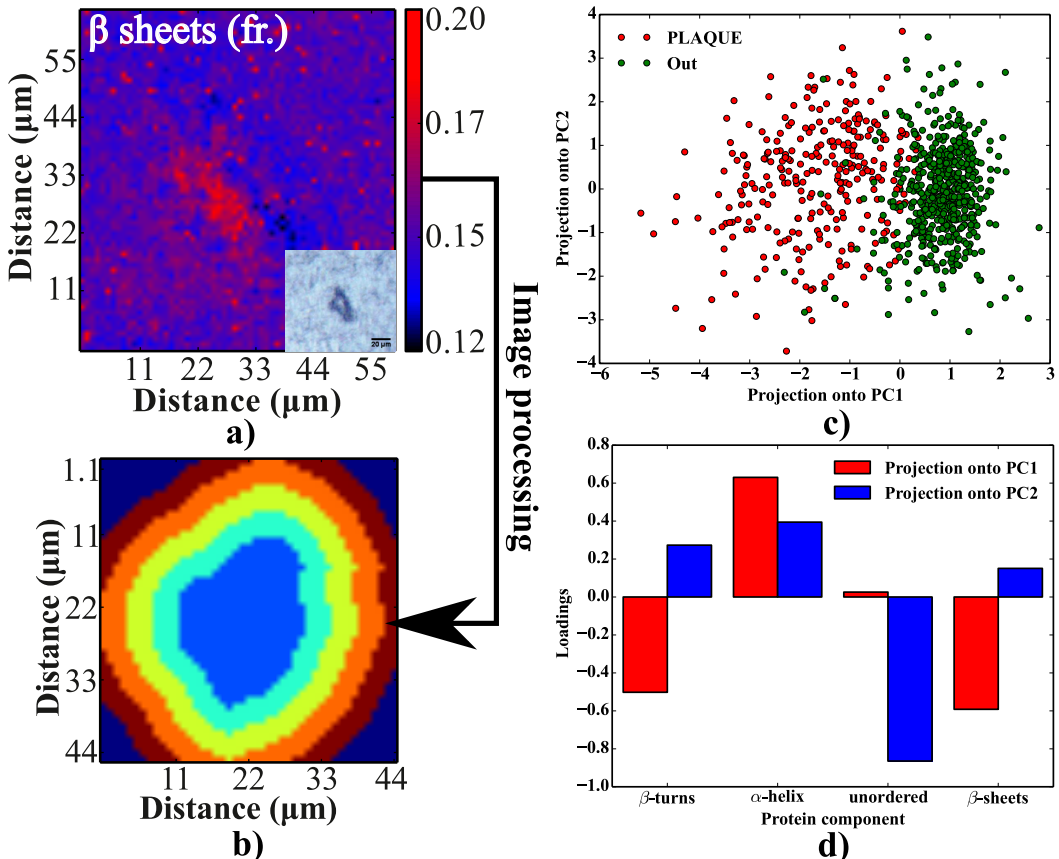

Fig. 13: a) FTIR image of the $A\beta$ deposit (β-sheets); b) processed image of the deposit; principal component analysis (PCA): c) projection of the data points onto the PCA1 vs. PC2 space; d) the corresponding loadings plot (PCA1, PCA2).

MLR-MR in FT-IR imaging [12]

Is an FT-IR spectrum always perfect?

For correcting against major obscuring effects in FT-IR microscopy a novel MLR-MR (ang. Multiple Linear Regression Multi-Reference), model was proposed:

$$z_{App}(\tilde{\nu}) = \underbrace{z_{bas}(\tilde{\nu})}_{\text{Baseline}} + \underbrace{z_{subs}(\tilde{\nu})}_{\text{Substrate}} + \underbrace{z_{fri}(\tilde{\nu})}_{\text{Fringes}} + \overbrace{z_{chem}(\tilde{\nu})}^{\text{Reference spectra}} + \underbrace{\epsilon(\tilde{\nu})}_{\text{Error}} \quad (9)$$

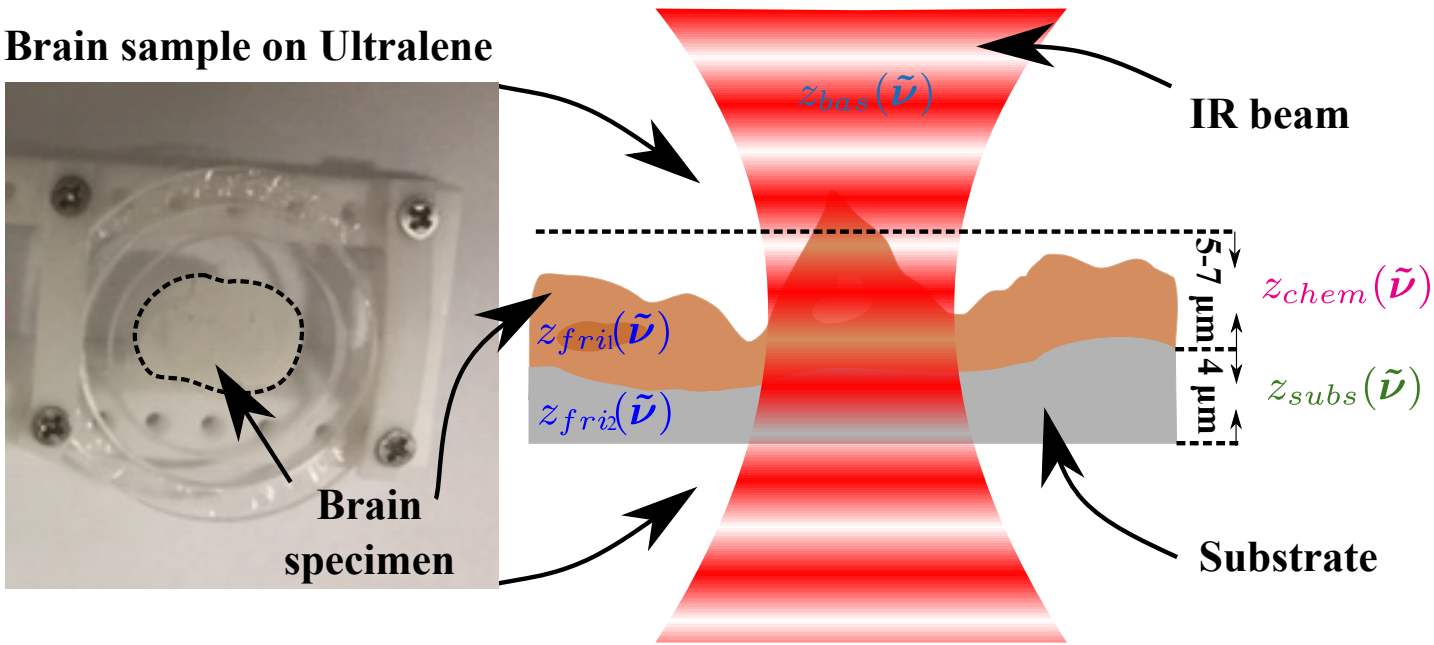

Fig. 14: Physical properties of analyzed tissue samples .

MLR-MR in FT-IR imaging [12]

Is an FT-IR spectrum always perfect?

For correcting against major obscuring effects in FT-IR microscopy a novel MLR-MR (ang. Multiple Linear Regression Multi-Reference), model was proposed:

$$z_{App}(\tilde{\nu}) = \underbrace{z_{bas}(\tilde{\nu})}_{\text{Baseline}} + \underbrace{z_{subs}(\tilde{\nu})}_{\text{Substrate}} + \underbrace{z_{fri}(\tilde{\nu})}_{\text{Fringes}} + \overbrace{z_{chem}(\tilde{\nu})}^{\text{Reference spectra}} + \underbrace{\epsilon(\tilde{\nu})}_{\text{Error}} \quad (9)$$

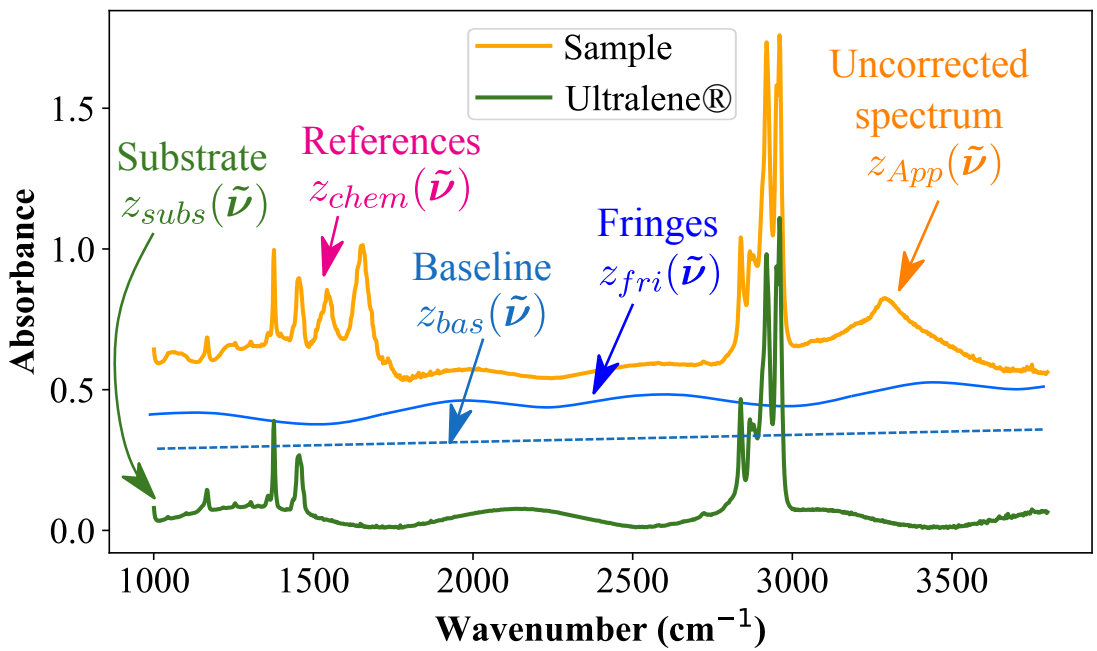

Fig. 14: Raw spectra from a single point.

MLR-MR in FT-IR imaging [12]

Is an FT-IR spectrum always perfect?

For correcting against major obscuring effects in FT-IR microscopy a novel MLR-MR (ang. Multiple Linear Regression Multi-Reference), model was proposed:

$$z_{App}(\tilde{\boldsymbol{\nu}}) = \underbrace{z_{bas}(\tilde{\boldsymbol{\nu}})}_{\text{Baseline}} + \underbrace{z_{subs}(\tilde{\boldsymbol{\nu}})}_{\text{Substrate}} + z_{fri}(\tilde{\boldsymbol{\nu}}) + z_{chem}(\tilde{\boldsymbol{\nu}}) + \epsilon(\tilde{\boldsymbol{\nu}})$$

$$z_{bas}(\tilde{\boldsymbol{\nu}}) = a + b \cdot \tilde{\boldsymbol{\nu}}$$

Constant and linear baseline effects

a - baseline offset;
b - baseline slope
$\tilde{\boldsymbol{\nu}}$ - the wavenumber vector $[cm^{-1}]$

$$z_{subs}(\tilde{\boldsymbol{\nu}}) = c \cdot U(\tilde{\boldsymbol{\nu}})$$

Structural variability of the substrate

c - a substrate contribution constant
$U(\tilde{\boldsymbol{\nu}})$ - the substrate (Ultralene®) spectrum

Conclusions

FT-IR microscopy is a versatile micro-spectro-chemical method allowing for:

- fast mapping and imaging of a variety of thin biological samples.
- analyzing chemical homogeneity of industrial materials in 3D.
- studying biochemistry/biophysics behind pathological states.

Despite great progress in instrumentation, there is still a gap in understanding major physical effects obscuring relevant spectral information!

Thanks!

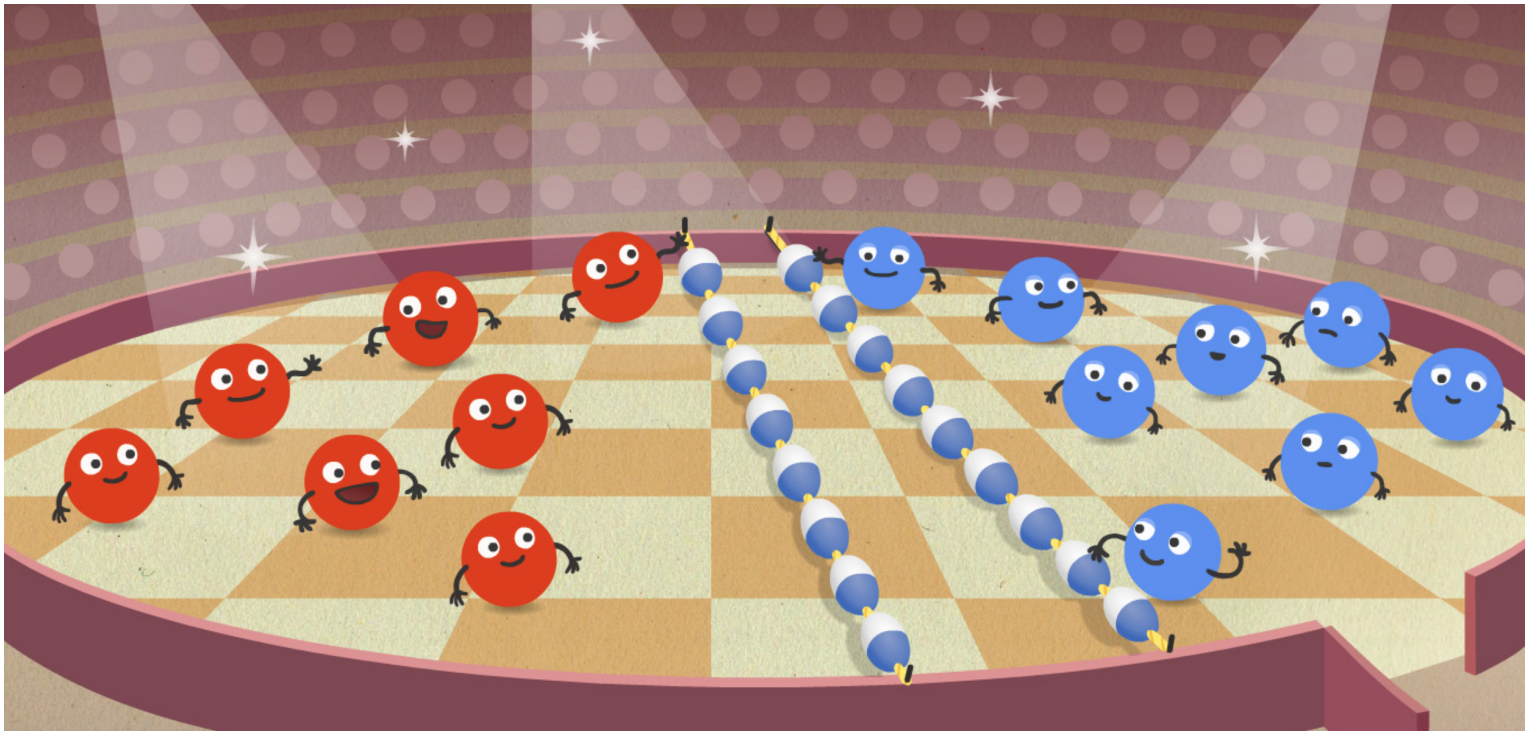

Fig. 14: Another artistic view on a molecular dance [6]

Thank You for Your attention!!!!

References I

[1] www.lotusgemology.com/images/library/articles/gemologyarticles/ftir-intrigue/infrared-spectrum.jpg, accessed on 2020-07-16.

[2] www.hyperphysics.phy-astr.gsu.edu/hbase/quantum/hosc.html, accessed on 2020-07-16, accessed on 2020-07-16.

[3] www.chemwiki.ucdavis.edu, accessed on 2020-07-16.

[4] www.shimadzu.com/an/ftir/support/tips/letter15/apodization.html, accessed on 2020-07-16.

[5] www.nicolet.co.uk/, accessed on 2020-07-16, accessed on 2020-07-16.

[6] www.concord.org/wp-content/uploads/2015/11/LOB-2a.png, accessed on 2020-07-16.

[7] Z. Kecki.
Podstawy spektroskopii molekularnej.
PWN, Warszawa, 1992.

[8] G. Smith.
Infrared microspectroscopy using a synchrotron source for arts-science research.
Journal of the American Institute for Conservation, 85(3):399–406, 2003.

[9] B. Stuart.
Infrared Spectroscopy: fundamentals and applications.
Wiley, 2004.

References II

[10] A. Surowka.
Development of analytical approaches for molecular and fully quantitative elemental micro-imaging of brain tissue with X-ray and infrared radiation.
AGH, 2016.

[11] A. Surowka, D. Adamek, and M. Szczerbowska-Boruchowska.
The combination of artificial neural networks and synchrotron radiation-based infrared micro-spectroscopy for a study on the protein composition of human glial tumors.
Analyst, pages 2428–38, 2015.

[12] A. Surowka, G. Birarda, M. Szczerbowska-Boruchowska, M. Cestelli-Guidi, A. Ziomber-Lisiak, and L. Vaccari.
Model-based correction algorithm for fourier transform infrared microscopy measurements of complex tissue-substrate systems.
Analytica Chimica Acta, pages 143–155, 2020.

[13] A. Surowka, M. Pilling, A. Henderson, H. Boutin, L. Christie, M. Szczerbowska-Boruchowska, and P. Gardner.
Ftir imaging of the molecular burden around a? deposits in an early-stage 3-tg-app-ps1-tau mouse model of alzheimer's disease.
Analyst, pages 156–168, 2016.